Available online at www.sciencedirect.com

Catalysis Today 137 (2008) 179–184

www.elsevier.com/locate/cattod

Selective reduction of NO_x by hydrogen and methane in natural gas stationary sources over alumina-supported Pd, Co and Co/Pd catalysts

Part A. On the effect of palladium precursors and catalyst pre-treatment

Rui Marques [a], Linda Mazri [a], Stéphanie Da Costa [b], Franck Delacroix [c], Gérald Djéga-Mariadassou [a], Patrick Da Costa [a,*]

[a] Université Pierre et Marie Curie (Paris 6), Laboratoire de Réactivité de Surface, CNRS UMR 7609, Case 178, 4 Place Jussieu, 75252 Paris Cedex 05, France

[b] Gaz de France, Direction de la Recherche, 361 Avenue du Président Wilson, B.P. 33, 93211 La Plaine Saint-Denis Cedex, France

[c] ADEME, 2 Square La Fayette, 49004 Angers, France

Abstract

The aim of the present work is to study the selective reduction of NO_x from natural gas sources. The unburned methane can be used as reductant. Another reductant such as hydrogen can be created in situ, using a microreformer. The results suggest that the NO_x are reduced by H_2 at low temperature, when methane is not activated and at higher temperature the methane is then the main reductant. However, the catalytic behaviour depends on the metal precursor and the catalyst treatment. The most prominent result is obtained on the palladium catalyst prepared from $Pd(NH_3)_4(NO_3)_2$ precursor. Comparing the reduction and the calcination step in the course of catalyst preparation, one can conclude that calcination lead to the higher activity in deNO_x, since reduced catalysts are oxidized during the deNO_x process.

Keywords: deNO_x; Hydrogen; Methane; Palladium precursor; Cationic species

1. Introduction

Nowadays, the harmful effects of emission of nitrogen oxides are completely recognized. Emission of NO_x ($NO + NO_2$) from vehicles and stationary sources are responsible for serious environmental problems. The deNO_x is the specific post-treatment for the reduction of nitrogen oxides present in the exhaust streams in lean-burn conditions. The SCR of NO_x by methane is a very attractive technology for the decreasing of NO_x from stationary sources, because natural gas (methane) is readily available.

Initially, Li and Armor [1] found that the most active catalysts for NO_x removal by methane in oxygen excess were based on cobalt supported on several zeolites. Bimetallic cobalt and palladium loaded zeolites exhibited much more resistance to water vapor than monometallic Co-zeolites [2–5]. Although they are more resistant, these catalysts also deactivate under long-term hydrothermal conditions. Another main obstacle of SCR of NO by methane is the low selectivity between the reaction with NO and O_2 [6,7]. This obstacle is important in the case of Pd, since Pd is very active for total oxidation of methane [8]. The used of Pd supported on acidic materials such as zeolites for he SCR of NO_x by methane, is correlated with the stabilization of the Pd^{2+} ions on acidic materials, which have low activity for methane oxidation [9]. Therefore, other acidic materials have been tested, such as sulphated zirconia and sulphated alumina [10,11]. Recently, a general three-function model for deNO_x catalysis [12–17] was also proposed for metals in cationic form. The authors claimed that three functions are necessary for the deNO_x process to occur: (i)

---

* Corresponding author. Tel.: +33 1 44 27 36 26; fax: +33 1 44 27 60 33.
E-mail address: dacosta@ccr.jussieu.fr (P. Da Costa).

0920-5861/$ – see front matter © 2007 Elsevier B.V. All rights reserved.
doi:10.1016/j.cattod.2007.11.025

oxidation of NO to NO_2; (ii) mild oxidation of methane to alcohol and aldehyde, in the presence of NO_2; (iii) reduction of NO to N_2, assisted by the deep oxidation of the alcohol and aldehyde to CO_2.

Moreover, many authors report that H_2 is a very effective reductant under lean conditions [18–23]. Pt and Pd based catalysts have been examined by Ueda et al. [19], for $H_2/NO/O_2$ reaction, under lean burn condition (5% O_2) in presence of 10% of H_2O. All Pd-based catalysts displayed two distinct conversion maxima for the reduction of NO, one centred at 100 °C and the second at 300 °C. At low temperature, the peak results from the reaction between H_2 and NO, while the peak at high temperature would be the result of the reaction between H_2 and NO_2 produces in situ. The maximum of NO_x conversion varies significantly with the choice of the support. Pd/TiO_2 shows the best activity, while for Pd/Al_2O_3, the total of NO_x conversion does not exceed 10%. Pieterse and Booneveld [22] reported the study of NO_x reduction by the reducing agents H_2, CO, CH_4, in presence and absence of O_2, H_2O and CO_2 on Zeolite MOR catalysts impregnated with palladium and cerium. This bimetallic catalyst provides high NO_x conversion showing high nitrogen selectivity (∼90%) with H_2 and CO under lean burn conditions, which is assigned to a synergic co-operation between CO and H_2. Engelmann-Pirez et al. [23] have showed that alumina- or perovskite-supported palladium catalysts are efficient for NO_x abatment in a mixture $H_2/NO/O_2$ at low temperature (<150 °C). The authors proposed that the active phase is metallic palladium. The influence of the precursor kind of catalysts on the course of NO_x reduction by CO has been investigated by Nazimek and Cwikla-Bundyra [24]. The authors showed that the NO_x reduction by CO depends on the kind of precursor. Indeed, $Pd(NO_3)_2$ precursor leads to the higher reactivity compared to chlorinated precursors. This paper reports a study on the influence of metal precursor and the influence of calcination or reduction on the SCR of NO_x by methane or hydrogen. Finally, the influence of methane and hydrogen used alone or both as reducing agents are studied.

2. Experimental

2.1. Catalysts synthesis

Catalysts were prepared by wet impregnation of crushed and sieved γ-Al_2O_3 ($0.8\ \text{mm} < d < 1.2\ \text{mm}$) (Procatalyse, specic surface area of 190 $m^2\,g^{-1}$, pore volume of 0.7 $cm^3\,g^{-1}$). Three different palladium precursors were used: (1) $Pd(NH_3)_4(NO_3)_2$ (5%) aqueous solution, (2) $Pd(NO_3)_2$ hydrate (99%), and (3) $PdCl_2$ hydrate (99%). The metal salts were dissolved to prepare the precursor suspension. To prepare the catalyst containing chloride, HCl (1 M) was used in order to dissolve the salt at RT in water. The pH of the solution was about 1.9.

The precursor's suspension was maintained under stirring at 333 K for 3 h. After complete removal of water by evaporation under reduced pressure, the catalysts were dried overnight with air at 393 K and calcined with air at 773 K for 2 h [16]. The as-prepared catalysts are labelled $Pd_{Pd(NH_3)_4)(NO_3)_2}$ $(X)/Al_2O_3$, $Pd_{PdCl_2}(X)/Al_2O_3$ and $Pd_{Pd(NO_3)_2}$ $(X)/Al_2O_3$.

2.2. Characterization of catalysts

The catalysts were characterized by XRD, transmission electron microscopy (TEM), and UV–visible–near-infrared (NIR). The specific surface area was also measured using a home made apparatus. Elemental analysis was performed by the "Service Central d'Analyses du CNRS" in order to determine the cobalt and palladium contents and cobalt-supported catalysts. Powder X-ray diffraction (XRD) was carried out on a Siemens model D-500 diffractometer with Cu Kα radiation. High-resolution transmission electron microscopy (HRTEM) was performed to determine the particle size of cobalt or palladium particles on alumina and to check their dispersion. HRTEM studies were performed on a JEOL-JEM 100 CXII apparatus associated with a top entry device and operating at 100 kV. EDS analysis was performed with the same apparatus using a LINK AN 10000 system, connected to a silicon–lithium diode detector, and multichannel analyser. EDS analyses were obtained on large domains of samples (150 nm × 200 nm to 400 nm × 533 nm). Diffuse reflectance spectra were recorded at room temperature between 190 and 2500 nm on a Varian Cary 5E spectrometer equipped with a double monochromator and an integrating sphere coated with polytetrafluoroethylene (PTFE). PTFE was the reference.

2.3. Catalytic measurements

The catalytic reaction was performed with the three reaction mixtures: (i) 150 ppm NO, 7 vol.% O_2, 0 vol.% CO_2, 9000 ppm CH_4, 0 vol.% H_2O, 0 ppm H_2, in Ar as balance; (ii) 150 ppm NO, 7 vol.% O_2, 0 vol.% CO_2, 0 ppm CH_4, 0 vol.% H_2O, 1500 ppm H_2, in Ar as balance; (iii) 150 ppm NO, 7 vol.% O_2, 0 vol.% CO_2, 9000 ppm CH_4, 0 vol.% H_2O, 1500 ppm H_2, in Ar as balance. The NO mixture was supplied by air liquide as 1 vol.% NO, and 99 vol.% Ar (<10 ppm other gases). The O_2 mixture contained 100 vol.% O_2 (air liquide). The CH_4 mixture contained 5 vol.% CH_4, and 95 vol.% Ar (air liquide). The total gas flow was maintained at 0.25 L min^{-1} NTP. Each of the gas mixtures was metered using calibrated electronic mass flow controllers (Brooks, Model 5850E). Taking a catalyst density of about 0.7 g/cm^3, the gas hourly space velocity (GHSV) was 50,000 h^{-1}. Catalytic experiments were carried out in a glass microreactor containing quartz wool supporting the sample. The bed temperature was measured using K-type thermocouple affixed to the outer reactor surface. The temperature was controlled using an electronic controller (Eurotherm 2408). The reactor outflow was analyzed using a set of specific detectors. An Eco Physics CLD 700 AL NO_x chemiluminescence analyzer (for NO and total NO_x (i.e. $NO + NO_2$)) allowed the simultaneous detection of NO, NO_2 and NO_x. An Ultramat 6 IR analyzer was used to monitor N_2O and a FID detector was used to follow the total concentration of hydrocarbons (HC). Temperature Programmed Desorption (TPD) experiments were carried out in Ar/O_2 (7 O_2 vol.% in Ar as balance, 0.250 L min^{-1}) with a heating rate of 5 °C min^{-1}, up to 500 °C, over pre-treated samples. Before TPD gas mixture was pre-adsorbed (150 ppm NO, 7 vol.% O_2 in Ar as balance, 0.250 L min^{-1}). Isothermal steady-state reaction was measured at different temperatures, ranging from 200 to 500 °C, in decreasing the temperature to avoid all the desorption effects. The NO_x and methane conversions were calculated from measured concentration of NO_x and methane, respectively.

3. Results and discussion

3.1. Highly dispersed cationic materials

The materials are characterized by XRD, no diffraction peaks of Pd are detected. Furthermore no crystallized phases are detected by HRTEM, although EDS showed Pd/Al ratios are constant. Palladium species are then highly dispersed on the support. Thus, UV–visible–NIR diffuse reflectance is performed to characterized theses latter species. The UV–visible–NIR diffuse reflectance spectra of $Pd_{PdCl2}(0.35)/Al_2O_3$, $Pd_{Pd(NO_3)_2}(0.35)/Al_2O_3$, $Pd_{(Pd(NH_3)_4)(NO_3)_2}(0.35)/Al_2O_3$ catalysts are displayed in Fig. 1. The spectra of the support consists mainly of several bands in the near-infrared (NIR) due to (i) $\nu_{(OH)}$ overtones of surface hydroxyl groups (1364 nm) and (ii) a combination of $\nu_{(OH)}$ and $\delta_{(OH)}$ (1885 and 2207 nm) [25]. Other bands are observed at ca. 420 nm for $Pd_{(Pd(NH_3)_4)(NO_3)_2}(0.35)/Al_2O_3$, and at 470 nm for $Pd_{PdCl_2}(0.35)/Al_2O_3$ and $Pd_{Pd(NO_3)_2}(0.35)/Al_2O_3$. The band located at 420 nm is characteristic of isolated Pd^{2+} in an oxygen environment and the band at 470 nm is characteristic of cationic palladium species in interaction with PdO nanoclusters [26]. As conclusion, no particles of PdO were detected. More over, in our samples, the palladium is well dispersed on the support. However, on $Pd_{(Pd(NH_3)_4)(NO_3)_2}(0.35)/Al_2O_3$, the palladium is only in cationic form whereas for $Pd_{PdCl_2}(0.35)/Al_2O_3$ and $Pd_{Pd(NO_3)_2}(0.35)/Al_2O_3$, the palladium is in cationic form or in PdO clusters form.

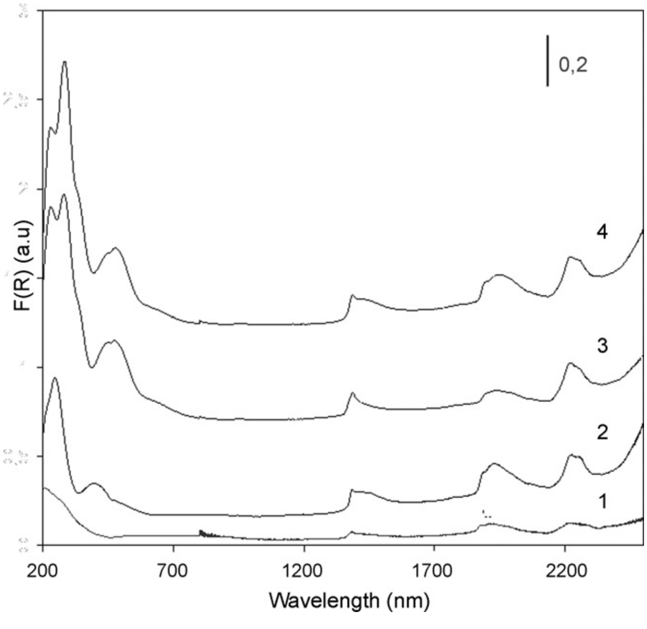

Fig. 1. UV–visible–NIR diffuse reflectance spectra of $Pd(X)/Al_2O_3$ catalysts (1) Al_2O_3, (2) $Pd_{(Pd(NH_3)_4)(NO_3)_2}(0.35)/Al_2O_3$, (3) $Pd_{PdCl_2}(0.35)/Al_2O_3$ and (4) $Pd_{Pd(NO_3)_2}(0.35)/Al_2O_3$.

3.2. Catalytic performance

3.2.1. NO, CH_4, O_2 reaction

The deNO_x catalytic behaviour was studied in steady-state conditions. The results of the three different catalysts contacted with NO, CH_4 and O_2 are presented in Fig. 2a. The deNO_x temperature window depends on the catalyst and thus on the palladium precursor.

A low deNO_x activity is obtained on Pd_{PdNO_3} (0.35)/Al_2O_3 from 250 to 400 °C. The maximum of conversion (7%) is observed at 350 °C. On Pd_{PdCl_2} (0.35)/Al_2O_3, the deNO_x temperature window is shifted at higher temperatures, i.e. from 350 to 500 °C, with a maximum of NO_x conversion of 13% at 500 °C. Finally, the highest activity, was obtained on $Pd_{(Pd(NH_3)_4)(NO_3)_2}(0.35)/Al_2O_3$, with about 50% of NO_x conversion to N_2 at 400 °C. More over, the deNO_x temperature window is from 250 to 500 °C. On this latter catalyst, the reduction of NO_x corresponds to temperature window of the second NO desorption peak. These results are in agreement with those obtained on alumina-supported catalysts [16]. For sake of comparison, on the support alone, no deNO_x activity and no methane consumption are observed in the studied temperature range (100–500 °C). Based on these results, one can conclude that the use of $Pd(NH_3)_4(NO_3)_2$ as precursor leads to the best catalyst in deNO_x SCR by methane. In the course of deNO_x reaction, the CO_2 concentration was followed in order to evaluate the oxidation properties of the catalysts. One can see in Fig. 2b that the methane is only transformed for temperatures in to CO_2 higher than 300 °C. Comparing the deNO_x and the oxidation activity, we can remark that these reactions do not take place in the same temperature range and that their respective rates are different. For Pd_{PdCl_2} (0.35)/Al_2O_3, the methane oxidation starts at 400 °C. At 500 °C, only 23% of methane is converted in CO_2. These results are in agreement with those observed by Roth et al. [27]. The authors have shown the inhibition effect of the chlorine on the catalyst. The elementary analyses show the presence of Chlorine after catalyst calcination and catalytic runs. Thus, on final Pd_{PdCl_2} (0.35)/Al_2O_3, the chlorine is still present and inhibits the methane oxidation. For $Pd_{(Pd(NH_3)_4)(NO_3)_2}(0.35)/Al_2O_3$, the methane conversion begins at 350 °C, and 100% of methane is converted at 500 °C. Finally, for Pd_{PdNO_3} (0.35)/Al_2O_3, the oxidation reaction starts at lower temperature in comparison with the other catalysts. Thus, the methane conversion starts at 300 °C and all methane is converted at 375 °C. The $Pd_{(Pd(NH_3)_4)(NO_3)_2}(0.35)/Al_2O_3$ presents a high selectivity in oxidation reaction. These results can be correlated with the characterizations. By UV–vis spectroscopy (Fig. 1) we show that the palladium is present as clusters in this catalyst. These PdO_x clusters are the active phase for the reaction of oxidation of methane [28]. Comparing the deNO_x and the oxidation activities, one can conclude that the catalysts which exhibit the higher oxidation activity present also the lower deNO_x activity. A correlation between deNO_x activity and methane oxidation can be proposed in agreement with the deNO_x model proposed by Djéga-Mariadassou et al. [12,13]. We have proposed on alumina-supported palladium catalysts that the reduction of NO_x occurs by the NO dissociation leading to N_2. During this process, one atom of oxygen is left on palladium sites.

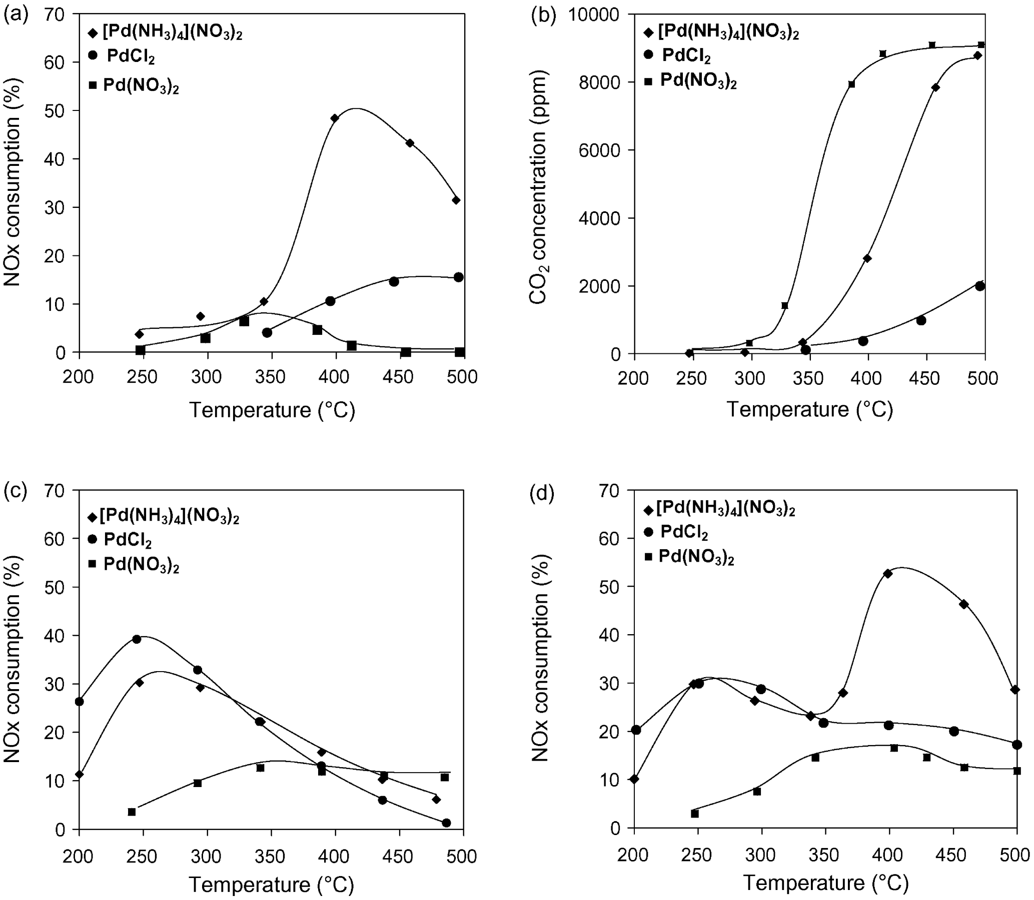

Fig. 2. (a) Isothermal steady-state consumption of NO_x in the course of CH_4–NO–O_2 (9000 ppm – 150 ppm – 7 vol.%), Ar as balance over: $Pd_{PdCl_2}(0.35)/Al_2O_3$, $Pd_{Pd(NO_3)_2}(0.35)/Al_2O_3$, $Pd_{(Pd(NH_3)_4)(NO_3)_2}(0.35)/Al_2O_3$; (b) evolution of CO_2 concentration during the isothermal steady-state consumption of NO_x in the course of CH_4–NO–O_2 (9000 ppm – 150 ppm – 7 vol.%), Ar as balance over: $Pd_{PdCl_2}(0.35)/Al_2O_3$, $Pd_{Pd(NO_3)_2}(0.35)/Al_2O_3$, $Pd_{(Pd(NH_3)_4)(NO_3)_2}(0.35)/Al_2O_3$; (c) isothermal steady-state consumption of NO_x in the course of H_2–NO–O_2 (1500 ppm – 150 ppm – 7 vol.%), Ar as balance over: $Pd_{PdCl_2}(0.35)/Al_2O_3$, $Pd_{Pd(NO_3)_2}(0.35)/Al_2O_3$, $Pd_{(Pd(NH_3)_4)(NO_3)_2}(0.35)/Al_2O_3$; (d) isothermal steady-state consumption of NO_x in the course of H_2–CH_4–NO–O_2 (1500 ppm – 9000 ppm – 150 ppm – 7 vol.%), Ar as balance over: $Pd_{PdCl_2}(0.35)/Al_2O_3$, $Pd_{Pd(NO_3)_2}(0.35)/Al_2O_3$, $Pd_{(Pd(NH_3)_4)(NO_3)_2}(0.35)/Al_2O_3$.

The methane by the intermediate of oxidized species such as formaldehyde [16] is oxidized to CO_2 through this "O" species. However, in the presence of oxygen (lean conditions), the methane is also oxidized through "O" species from the oxygen dissociation on palladium sites. Thus, the oxidized species of methane or the methane itself is oxidized by "O" species from NO or from O_2. A kinetic coupling between CH_4/NO and CH_4/O_2 reactions can then be proposed on palladium sites. This coupling was recently reported by Musi et al. [29] with EtOH. Thus a coupling was found between EtOH/NO and EtOH/O_2 reactions on other cationic systems. If we propose that the global rate of CO_2 formation is the sum of the rate of deNO_x reaction and the rate of methane oxidation ($r_{g,CO_2} = r_{NO} + r_{O_2}$). The difference of de$NO_x$ activity between precursors is easily understandable. For $Pd_{PdCl_2}(0.35)/Al_2O_3$, as the overall rate of CO_2 formation is low ($r_{g,CO_2} = r_{NO} + r_{O_2}$), thus the rate r_{NO} is also low. This can be explained by the presence of chlorine on the catalyst. For $Pd_{PdNO_3}(0.35)/Al_2O_3$, the overall rate is high. However, the deNO_x rate is low, thus the oxidation rate r_{O_2} is then high. This high selectivity for total oxidation of methane is due to palladium species, such as palladium oxide clusters that are active sites for oxidation reactions. These clusters are not active for deNO_x process. Finally, the $Pd_{(Pd(NH_3)_4)(NO_3)_2}(0.35)/Al_2O_3$ catalyst, that presents a high activity in the temperature range expected by TPD's experiments, is the one in which palladium is only present as Pd^{2+} surrounded by oxygen. These cationic species are then responsible for deNO_x activity.

3.2.2. NO, H_2, O_2 reaction

After the study of SCR of NO_x by methane, the same catalysts are used in presence of 150 ppm of NO, 1500 ppm of H_2 and 7% of O_2 in presence of argon as carrier gas. The results are presented in Fig. 2c. The NO_x consumption depends on the palladium precursor. 10% of NO_x conversion is found for $Pd_{PdNO_3}(0.35)/Al_2O_3$ catalyst from 350 to 500 °C. The temperature range of NO_x conversion increases when the two other precursors are used. In that case, a NO_x conversion is observed from 200 to 450 °C. More over, the maximum of deNO_x depends on the precursor. For $Pd_{(Pd(NH_3)_4)(NO_3)_2}(0.35)/Al_2O_3$ catalyst, 30% of deNO_x is observed at 250 °C whereas about 40% of NO_x conversion is obtained at the same temperature on $Pd_{PdCl_2}(0.35)/Al_2O_3$ catalyst. However, $Pd_{(Pd(NH_3)_4)(NO_3)_2}(0.35)/Al_2O_3$ catalyst deactivates with time on stream and the NO_x conversion reaches 30% after catalyst deactivation. After runs, the palladium catalysts were characterized by UV–vis spectroscopy. No significant differences are obtained from fresh and used catalysts. Thus we can conclude that the actives sites in our reaction conditions are palladium species such as Pd^{2+} surrounded by oxygen atoms.

3.2.3. NO, H_2, CH_4, O_2 reaction

A subsequent reaction with a complete mixture containing 150 ppm of NO, 1500 ppm of H_2, 9000 ppm of CH_4 and 7% of O_2 was performed in the same catalysts in order to compare the deNO$_x$ activity in presence of both hydrogen and methane with the deNO$_x$ activity in presence of methane or hydrogen in the feed.

The results are presented in Fig. 2d. Two maxima for NO$_x$ conversion were obtained on $Pd_{(Pd(NH_3)_4)(NO_3)_2}$ catalyst in the range of the studied temperature (200–500 °C). These two maxima are located at 250 °C (30% of conversion) and 400 °C (53% of conversion). The first maximum is assigned to the presence of hydrogen and the second one to the presence of methane. These results are in agreement with those obtained by Pieterse and Booneveld [22] on cobalt palladium zeolitic catalysts. Comparing Fig. 2a, c and d, one can see that the deNO$_x$ activity in presence of complete mixture is the sum of those obtained with methane and with hydrogen. Thus, in increasing the concentration in reductant, the deNO$_x$ activity is enhanced, even if the reductant is different and acts at different temperature range. The same conclusions can be drawn on $Pd_{Pd(NO_3)_2}$ catalyst (Fig. 2d). However, the catalyst prepared from PdCl2 loses deNO$_x$ activity at low temperature. After deactivation, almost 30% of NO$_x$ conversion is observed at 250 °C. Thus, methane and hydrogen used together leads to a large range of temperature for deNO$_x$ conversion. On all catalyst, we proposed that both in presence of methane and hydrogen, the active sites should be palladium in Pd^{2+} form. To verify this point, we have decided to reduce a catalyst and to compare this one to those was calcinated before test.

3.3. Reduced catalysts

A calcinated $Pd_{(Pd(NH_3)_4)(NO_3)_2}$ catalyst was reduced in situ before reaction, in flowing 20% hydrogen in Ar (100 $cm^3\,min^{-1}$) through the catalyst from RT to 500 °C with a heating rate of 3 $°C\,min^{-1}$. The results of deNO$_x$ studies, $CH_4/NO/O_2$, $H_2/NO/O_2$, $CH_4/H_2/NO/O_2$, respectively are presented in Fig. 3. In presence of methane alone, the NO$_x$NO$_x$ in N_2 starts at 300 °C and about 50% of NO$_x$ conversion is observed at 400 °C. In presence of hydrogen, a maximum of NO$_x$ conversion is obtained at 300 °C. On calcinated catalyst the maximum of NO$_x$ conversion was obtained at lower temperature. With both reductants, the maxima are obtained at 250 and 400 °C. These results are close to those obtained on calcinated $Pd_{(Pd(NH_3)_4)(NO_3)_2}$ catalyst and leads us to think that the reduced catalyst is oxidized in the course of deNO$_x$ process in presence of 7% of O_2. UV–vis characterization performed after runs shows a band at around 400 nm (figure not shown). Thus, one can conclude that the reduced palladium becomes oxidized during the deNO$_x$ process. After runs, the active sites are palladium species: Pd^{2+} surrounded of oxygen atoms.

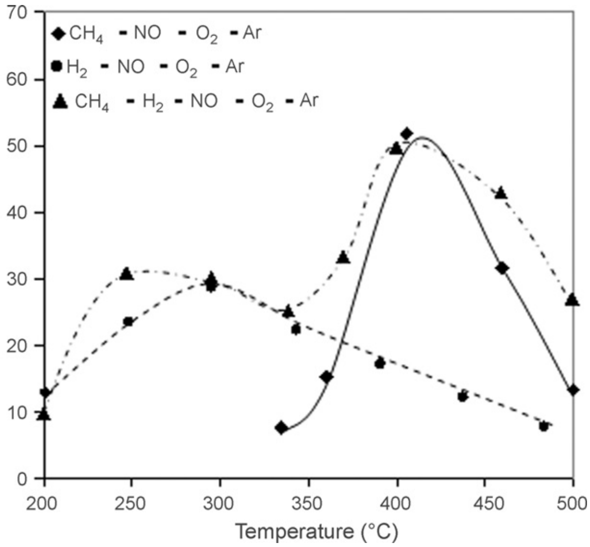

Fig. 3. Isothermal steady-state consumption of NO$_x$ in the course of CH_4–NO–O_2 (9000 ppm – 150 ppm – 7 vol.%) or H_2–NO–O_2 (1500 ppm – 150 ppm – 7 vol.%) or H_2–CH_4–NO–O_2 (1500 ppm – 9000 ppm – 150 ppm – 7 vol.%), Ar as balance over: $Pd_{(Pd(NH_3)_4)(NO_3)_2}(0.35)/Al_2O_3$, after reduction at 500 °C 2 h (20 $cm^3\,h^{-1}$ H_2, 80 $cm^3\,h^{-1}$).

4. Conclusions

Alumina-supported palladium catalysts were tested for NO reduction by methane and by hydrogen. The influence of palladium precursor was studied and leads to conclude that $Pd_{(Pd(NH_3)_4)(NO_3)_2}$ catalyst is the more active in presence of methane and in presence of hydrogen. The ranking of activity is the following in presence of methane: $Pd_{(Pd(NH_3)_4)(NO_3)_2}$ catalyst > Pd_{PdCl_2} catalyst > $Pd_{Pd(NO_3)_2}$ catalyst; in presence of hydrogen: $Pd_{(Pd(NH_3)_4)(NO_3)_2}$ catalyst = Pd_{PdCl2} catalyst > $Pd_{Pd(NO_3)_2}$ catalyst. The as prepared catalyst is stable during time of stream in comparison to that prepared from chlorine precursor which deactivates with time. The preformed studies were done in absence of water. In presence of 2% of water in the feed with $Pd_{(Pd(NH_3)_4)(NO_3)_2}$ catalyst, the NO$_x$ conversion decreases of about 10%. At 400 °C, on this catalyst, 45% of NO$_x$ conversion is observed. However, the inhibiting effect of water is reversible. On all the studied catalysts, the palladium was found to be in a form such as Pd^{2+} surrounded by oxygen atoms. On Pd_{PdCl_2} catalyst, the chlorine is also found on the catalyst, leading to a lower activity in deNO$_x$. Finally, on $Pd_{Pd(NO_3)_2}$ catalyst, the palladium is in Pd^{2+} in interaction with PdO cluster, leading to higher oxidizing properties and thus lower deNO$_x$ activity. By TEM, no palladium oxide particles are detected even if at high resolution. By EDS, palladium/aluminium ratios are constant. The palladium is then well dispersed on the support. The active phase for deNO$_x$ process is then Pd^{2+} surrounded by oxygen atoms. This conclusion is comforted by the experiments performed in the presence of reduced alumina-supported palladium catalysts. Indeed, metallic palladium particles are oxidized in the course of deNO$_x$ reaction even if presence of 1500 ppm of hydrogen. And after runs, Pd^{2+} phases were found by UV–vis spectroscopy.

Based on these results, cobalt-palladium bimetallic catalysts were synthesized using tetramine nitrate palladium as palladium precursor. The as prepared catalysts were then tested using the same methodology. Moreover, deNO$_x$ experiments in presence of 10 ppm of SO$_2$ are in course to evaluate the thioresistance of the prepared catalysts. More over, these actives phases will be washcoated on a cordierite supported to be test at syngas pilot scale.

Acknowledgements

This work was carried out in the framework of the European program ‘‘EUREKA’’ STATIONOCAT. Rui Marques acknowledges the financial support of ADEME and Gaz de France in the form of an ‘‘ADEME’’ grant. Prof. Bozon-Verduraz and Dr. P. Beaunier are greatly acknowledged for UV–vis and TEM experiments, respectively.

References

[1] Y. Li, J. Armor, J. Catal. 150 (1994) 376.
[2] L.F. Cordoba, G.A. Fuentes, C. Montes de Correa, Micropor. Mesopor. Mater. 77 (2005) 193.
[3] F. Bustamante, F. Córdoba, M. Yates, C. Montes de Correa, Appl. Catal. A 234 (2002) 127.
[4] M. Ogura, Y. Sugiura, M. Hayashi, E. Kikuchi, Catal. Lett. 42 (1996) 185.
[5] M. Ogura, S. Kage, T. Shimojo, J. Oba, M. Hayashi, M. Matsukata, E. Kikuchi, J. Catal. 211 (2002) 75.
[6] M. Iwamoto, H. Yahiro, Catal. Today 22 (1994) 5.
[7] M. Iwamoto, H. Hamada, Catal. Today 10 (1991) 57.
[8] C.J. Loughran, D.E. Resasco, Appl. Catal. B 7 (1995) 113.
[9] Y.-H. Chin, A. Pisanu, L. Serventi, W.E. Alvarez, D.E. Resasco, Catal. Today 54 (1999) 419.
[10] N. Li, A. Wang, L. Ren, M. Zheng, X. Wang, T. Zhang, Top. Catal. 30/31 (2004) 103.
[11] N. Li, A. Wang, M. Zheng, X. Wang, R. Cheng, T. Zhang, J. Catal. 225 (2005) 307.
[12] G. Djéga-Mariadassou, M. Boudart, J. Catal. 216 (2003) 89.
[13] G. Djéga-Mariadassou, Catal. Today 90 (2004) 27.
[14] C. Thomas, O. Gorce, C. Fontaine, J.-M. Krafft, F. Villain, G. Djéga-Mariadassou, Appl. Catal. B 63 (2006) 201.
[15] A.P. Ferreira, S. Capela, P. Da Costa, C. Henriques, M.F. Ribeiro, F.R. Ribeiro, Catal. Today 119 (2007) 156.
[16] R. Marques, K. El kabouss, P. Da Costa, S. Da Costa, F. Delacroix, G. Djéga-Mariadassou, Catal. Today 119 (2007) 166.
[17] F. Baudin, P. Da Costa, C. Thomas, S. Calvo, Y. Lendresse, S. Schneider, F. Delacroix, G. Plassat, G. Djéga-Mariadassou, Top. Catal. 30/31 (2004) 97.
[18] K. Yokota, M. Fukui, T. Tanaka, Appl. Surf. Sci. 121/122 (1997) 273.
[19] A. Ueda, N. Takayuki, A. Masashi, T. Kobayashi, Catal. Today 45 (1998) 135.
[20] N. MacLeod, R.M. Lambert, Appl. Catal. B 35 (2002) 269.
[21] N. MacLeod, R.M. Lambert, Appl. Catal. B 46 (2003) 483.
[22] J.A.Z. Pieterse, S. Booneveld, Appl. Catal. B 73 (2007) 350.
[23] M. Engelmann-Pirez, P. Granger, G. Leclercq, Catal. Today 107 (2005) 315.
[24] D. Nazimek, W. Cwikla-Bundyra, Catal. Today 90 (2004) 39.
[25] K. El kabouss, M. Kacimi, M. Ziyad, S. Ammar, F. Bozon-Verduraz, J. Catal. 226 (2004).
[26] D. Tessier, A. Rakai, F. Bozon-Verduraz, J. Chem. Soc., Faraday Trans. 88 (1992) 741.
[27] D. Roth, P. Gélin, M. Primet, E. Tena, Appl. Catal. A 203 (2000) 37.
[28] P. Gélin, L. Urfels, M. Primet, E. Tena, Catal. Today 83 (2003) 45.
[29] A. Musi, D. Broszki, J.M. Trichard, G. Djéga-Mariadassou, P. Da Costa, Catal. Today, submitted for publication, this volume.